Biometrical Journal **42** (2000) 7, 901–916

# An Approach to Quantifying the Multi-Channel EEG Spatial-Temporal Feature

PEI-CHEN LO and WEN-PO CHUNG

Department of Electrical and Control Engineering
National Chiao Tung University
Taiwan
Republic of China

*Summary*

Investigation of spatial characteristics in the multi-channel EEG (electroencephalogram) has been of great importance to the fundamental and clinical medicine. Conventional methods are mostly based on the coherence and correlation analysis in time and frequency domain. The authors present the method of quantifying the global waveform complexity in EEG by analyzing the high-dimensional state-space trajectory constructed from the multi-channel EEG. The resulting average complexity index ($\bar{\delta}$) is well distinct between the background ($4.0 \sim 4.5$) and event ($3.0 \sim 3.5$ for the focal-sharp-wave transient) in the 5-channel case study. In addition, the running $\bar{\delta}$ measurement for different electrode arrays, for a fixed number of state-space dimension ($n = 5$), reveals the EEG spatial characteristic. An array composed of nearby channels with similar EEG activities tends to have a small $\bar{\delta}$. On the other hand, the computed $\bar{\delta}$ increases as the array consists of electrode sites with spatially incorrelated EEG activities. Thus the method is capable of quantifying the spatial-temporal feature of the multi-channel EEG.

*Key words:* Multi-channel EEG (electroencephalogram); Spatial-temporal feature; State-space trajectory; Intrinsic dimension; Complexity index; Global waveform complexity.

## 1. Introduction

For decades, the electrical activity of the human brain (electroencephalogram, EEG) has been extensively studied in order to help clinicians diagnose and treat brain disfunctions. To deal with an enormous amount of recorded EEG, data quantification has been the primary step of EEG analysis. A number of methods have been developed to quantify the EEG. They can be generally classified as time-domain, frequency-domain, and other techniques (VAN GILS et al., 1997). Among many other techniques, methods based on the nonlinear dynamical theory have been used to quantify the underlying brain dynamics and evaluate the EEG wave-

form complexity since more than one decade ago (Babloyantz and Destexhe, 1986; Lo and Principe, 1989; Rapp et al., 1989; Pijn et al., 1991). Nonetheless, tools from nonlinear dynamical theory used for EEG analysis, such as the dimensional computation and Lyapunov exponent estimation, mostly suffer from the problems of computational inefficiency and bias from implementing parameters (Lo and Principe, 1989). Thus they are not feasible for long-term monitoring or practical use. Yaylali, Koçak, and Jayakar (1996) proposed a method that estimated the correlation dimension of unbiased autocovarianced EEG signals. They proved their technique to be computationally robust with respect to implementing parameters. Yet the method was develop to analyze a single EEG channel. The spatial EEG features over the scalp surface are of great importance. Wackermann et al. (1993) suggested viewing the *n*-channel EEG data as a trajectory in *n*-dimensional state space. Then the 'global' correlation dimension was evaluated. Since evaluating the correlation dimension involves slope computation using linear regression, an appropriate linear scaling region needs to be determined first. The estimation procedure is an indirect approach. Thus it is not feasible for the long-term, multi-channel EEG analysis.

The topological or intrinsic dimensionality of a point set was introduced to characterize the classifiers in the field of pattern recognition (Fukunaga and Olsen, 1971; Pettis et al., 1979; Verveer and Duin, 1995; Bruske and Sommer, 1998). The fundamental idea of its application to EEG analysis is that the intrinsic dimensionality in some sense reflects variation of data structure in a data set. Accordingly, we adapt the technique for the multi-channel EEG analysis to explore the spatial-temporal characteristics in EEG. To improve the computational efficiency, methods for determining the intrinsic dimension were mostly based on the local approaches, that is, quantifying the local features in small regions. The local intrinsic dimensionality (Fukunaga and Olsen, 1971; Passamante and Farrell, 1991; Michel and Flandrin, 1993) can be estimated by: 1) eigenvalue analysis or principal-component analysis (PCA), and 2) *K*'s nearest neighborhood (*K*NN) analysis. When applying to the long-term biomedical signals, computational efficiency and processing effectiveness are of important consideration. Thus the authors develop a direct-computation algorithm, based on the *K*NN approach, to analyze the multi-channel EEG. The algorithm avoids the problem of sophisticated computation strategy usually involved in indirect approach like the correlation dimension estimation. The mathematical basis is similar to that given in (Fuga and Flick, 1984). The derivation and implementation procedures are somewhat different. Hence the estimated result is to be called "complexity index (δ)".

## 2. Evaluation of Complexity Index

As previously demonstrated (Lo and Principe, 1989), the EEG trajectory forms a strange attractor (Hentschel and Procaccia, 1983). Let $\boldsymbol{X} = \{\boldsymbol{X}_i\}_{i=1}^{N}$ be the

points on the EEG trajectory, where $\boldsymbol{X}_i$ is an $n$-dimensional point constructed from the $n$-channel EEG signals. For instance, $\boldsymbol{X}_i$ = (F3($i$), Fz($i$), F4($i$)) represents a point on the 3-dimensional space, whose coordinates (degrees of freedom) are brain electrical potentials recorded from sites F3, Fz, and F4, respectively. For each point in the set $\boldsymbol{X}$ (e.g., $\boldsymbol{X}_i$), a $K$NN hypersphere is determined and formed by the $K$'s nearest neighboring (NN) points $\{\boldsymbol{V}_{ij}\}_{j=1}^{K}$, $\boldsymbol{V}_{ij} \in \boldsymbol{X}$ and $\boldsymbol{V}_{i1} = \boldsymbol{X}_i$. The $\boldsymbol{X}_i$ is called the seed point of the $i$th hypersphere. Inside the $i$th hypersphere, the largest distance to the seed point $\boldsymbol{X}_i$ is:

$$d_{i,K\mathrm{NN}} = \|\boldsymbol{X}_i - \boldsymbol{V}_{iK}\| \tag{1}$$

where the operator $\|\cdot\|$ evaluates the Euclidean distance. FUKUNAGA and FLICK (1984) analyzed the pattern classification error and obtained

$$\frac{E\{d_{(K+1)\,\mathrm{NN}}\}}{E\{d_{K\mathrm{NN}}\}} = 1 + \frac{1}{Kn} \tag{2}$$

where $E\{d_{K\mathrm{NN}}\}$ is the first order moment of $d_{K\mathrm{NN}}$. The $d_{K\mathrm{NN}}$ denotes the $K$th NN distance of any hypersphere in $\boldsymbol{X}$. The equation points out the effect of $K$ on classification error for a given number of space dimension $n$. Derivation of eq. (2) was based on the concept that the probability of $\boldsymbol{X}$ being inside the $i$th hypersphere is:

$$\mu = P(\boldsymbol{X}_i) \cong p(\boldsymbol{X}_i) \cdot \upsilon_{i,K\mathrm{NN}} = p(\boldsymbol{X}_i) \cdot (\alpha \times d_{i,K\mathrm{NN}}^{n}) \tag{3}$$

where $p(\boldsymbol{X}_i)$ is the probability density function and $\upsilon_{i,K\mathrm{NN}} = \alpha \times d_{i,K\mathrm{NN}}^{n}$ is the volume of the $i$th hypersphere. The coefficient $\alpha$ is the amending factor in computing the hyperspherical volume from the $n$th power of distance $d_{i,K\mathrm{NN}}$. The probability density $p(\boldsymbol{X}_i)$ depends on the distribution of $\boldsymbol{X}$. The first order moment of the $K$th NN distance of the $i$th hypersphere, $E\{d_{i,K\mathrm{NN}}\}$, can be obtained by substituting $d_{i,K\mathrm{NN}} = \mu^{1/n}(\alpha \cdot p(\boldsymbol{X}_i))^{-1/n}$. Then the first order moment of $d_{K\mathrm{NN}}$, $E\{d_{K\mathrm{NN}}\}$, is computed by taking the expectation of $E\{d_{i,K\mathrm{NN}}\}$ with respect to $\boldsymbol{X}_i$. Detailed derivation can be found in (FUKUNAGA and FLICK, 1984).

FUKUNAGA and FLICK aimed at quantifying the pattern classification error in the $K$NN model. They hypothesized an $n$-dimensional space for the pattern vectors, where $n$ is an integer. In order to quantify the global waveform complexity of multi-channel EEG, we apply the concept of fractional dimensionality of a strange attractor. Then the volume of the $i$th hypersphere can be estimated by

$$\upsilon_{i,K\mathrm{NN}} = \frac{\mu}{p(\boldsymbol{X}_i)} \cong \alpha \times d_{i,K\mathrm{NN}}^{\delta} \tag{4}$$

where $\delta$ is the complexity index of the trajectory to be evaluated in this study. And $\delta$ may be a fractional number. The first-order moment of $d_{i,K\mathrm{NN}}$ for a given $\boldsymbol{X}_i$ is

$$E\{d_{i,K\mathrm{NN}}\} \cong E\left\{\left(\frac{\mu}{\alpha p(\boldsymbol{X}_i)}\right)^{1/\delta}\right\} = \int_0^1 \left(\frac{\mu}{\alpha p(\boldsymbol{X}_i)}\right)^{1/\delta} p(\mu)\,\mathrm{d}\mu\,, \tag{5}$$

where the probability density function $p(\mu)$ is (Fraser, 1957)

$$p(\mu) = \frac{N!}{(K-1)!\,(N-K)!}\,\mu^{K-1}(1-\mu)^{N-K}\,. \tag{6}$$

Substituting eq. (6) into eq. (5) leads to an estimate of $E\{d_{i,K\mathrm{NN}}\}$ as

$$\begin{aligned} E\{d_{i,K\mathrm{NN}}\} &\cong (\alpha p(\boldsymbol{X}_i))^{-1/\delta}\frac{N!}{(K-1)!\,(N-K)!}\int_0^1 \mu^{K+1/\delta-1}(1-\mu)^{N-K}\,\mathrm{d}\mu \\ &= (\alpha p(\boldsymbol{X}_i))^{-1/\delta}\frac{N!}{(K-1)!\,(N-K)!}\,\frac{\Gamma(K+1/\delta)\cdot\Gamma(N-K+1)}{\Gamma(N+1/\delta+1)} \end{aligned} \tag{7}$$

where $\Gamma(\cdot)$ is the gamma function. Since $\Gamma(K) = (K-1)!$, eq. (7) becomes

$$\begin{aligned} E\{d_{i,K\mathrm{NN}}\} &\cong (\alpha p(\boldsymbol{X}_i))^{-1/\delta}\,\frac{\Gamma(N+1)}{\Gamma(K)\cdot\Gamma(N-K+1)}\,\frac{\Gamma(K+1/\delta)\cdot\Gamma(N-K+1)}{\Gamma(N+1/\delta+1)} \\ &= (\alpha p(\boldsymbol{X}_i))^{-1/\delta}\,\frac{\Gamma(N+1)}{\Gamma(K)}\,\frac{\Gamma(K+1/\delta)}{\Gamma(N+1/\delta+1)} \end{aligned} \tag{8}$$

which can be further reduced to

$$E\{d_{i,K\mathrm{NN}}\} \cong (\alpha p(\boldsymbol{X}_i))^{-1/\delta}\,\frac{\Gamma(K+1/\delta)}{\Gamma(K)} \tag{9}$$

given that $N \gg 1/\delta$. Taking the first-order expectation, with respect to $\boldsymbol{X}_i$, of eq. (9) results in

$$E\{d_{K\mathrm{NN}}\} \cong \alpha^{-1/\delta}E\{p^{-1/\delta}(\boldsymbol{X}_i)\}\,\frac{\Gamma(K+1/\delta)}{\Gamma(K)}\,. \tag{10}$$

To eliminate the factor of $p(\boldsymbol{X}_i)$ in computing $\delta$, the algorithm actually evaluates the ratio of $E\{d_{(K+1)\mathrm{NN}}\}$ to $E\{d_{K\mathrm{NN}}\}$. Since

$$\frac{E\{d_{(K+1)\,\mathrm{NN}}\}}{E\{d_{K\mathrm{NN}}\}} \cong \frac{\Gamma(K+1+1/\delta)}{\Gamma(K+1)}\frac{\Gamma(K)}{\Gamma(K+1/\delta)} = \frac{K+1/\delta}{K} = 1+\frac{1}{K\delta} \tag{11}$$

it follows that

$$\delta = \frac{1}{K}\left(\frac{E\{d_{(K+1)\,\mathrm{NN}}\}}{E\{d_{K\mathrm{NN}}\}} - 1\right)^{-1} \tag{12}$$

which provides the way to evaluate the complexity index.

One advantage of the method is its easy implementation of the algorithm by following eq. (12). The algorithm first determines a 2-dimensional $N \times N$ array $\boldsymbol{D}$ with its elements $d_{ij}$, $i, j = 1,\ldots, N$ representing the inter-point distances. Then elements in each row are sorted according to their magnitudes. The resulting $N \times N$ array $\boldsymbol{D}' = [d'_{ij}]$ $i, j = 1,\ldots, N$ has its elements in each row arranged from the

smallest ($j = 1$) to the largest ($j = N$) number. Thus the $K$th element of the $i$th row of $\boldsymbol{D}'$ is the $d_{i,K\mathrm{NN}}$. (i.e., $d_{i,K\mathrm{NN}} = d'_{iK}$) The algorithm actually compute the $E\{d_{K\mathrm{NN}}\}$ by averaging all the elements in the $K$th column of $\boldsymbol{D}'$. Likewise, the $E\{d_{(K+1)\mathrm{NN}}\}$ can be computed by averaging all the elements in the $(K+1)$th column of $\boldsymbol{D}'$. The complexity index $\delta$ is then computed by using eq. (12). Note that, due to limitation of memory capacity, the algorithm may not be able to store the $N \times N$ array if the size $N$ is large. In that case, the implementing procedure can be designed on the row-by-row basis, that is, obtaining $d_{i,K\mathrm{NN}}$ and $d_{i,(K+1)\,\mathrm{NN}}$ for each row without storing the other irrelevant inter-point distances. The disadvantage is the doubling of computer time spent on computing all the inter-point distances.

The computer time can be further reduced by modifying the sorting process as follows. Consider the $i$th row, that is, the seed point is $\boldsymbol{X}_i$. The algorithm in the beginning sorts the first $(K+1)$ inter-point distances, $d_{ij}$, $j = 1, \ldots, (K+1)$, and keeps them in sequence in a data buffer. Let $[d'_{ij}]$, $j = 1, \ldots, (K+1)$ represent the sorted data array, i.e. $d'_{im} \leq d'_{in}$ if $1 \leq m < n \leq (K+1)$. Each of the remaining distances, $d_{ij}$, $j = (K+2), \ldots, N$, is then compared with every element in the data buffer. If $d_{ij}$ is smaller than one of the elements in the data buffer (e.g., $d'_{im}$), $d_{ij}$ is inserted in the $m$th position and the $d'_{i(K+1)}$ is excluded from the buffer. The competition process is performed on each newly computed inter-point distance. Finally, the data buffer stores the smallest $(K+1)$'s distances. Undoubtedly, computer time required by the algorithm implemented in this manner is highly dependent on the value of $K$. A large $K$ costs more effort in the competition process. The overall computer time is less than that required by the previous algorithm.

## 3. Considerations in Evaluating Complexity Index

For the model systems with known system equations, complexity index can be evaluated from the model-generated trajectory. Thus the estimated $\delta$ depends on value of $K$ and length of the evolving trajectory. Figure 1 plots the estimated $\delta$ for $1 \leq K \leq 100$ for five model systems. The evolving length and time step used to generate each trajectory are listed in Table 1. As shown in Figure 1, the estimated $\delta$ reaches a steady value when $K \geq 10$. Note that the $\delta$ versus $K$ curves fluctuate. Thus the authors average the $\delta$'s over a moderate range of values of $K$ to obtain the final estimate. The average $\delta$ is denoted by $\bar{\delta}$. As listed in Table 1, the values of $K$ used to obtain $\bar{\delta}$ range from 30 to 60. Table 1 also lists the correlation dimension estimated for each model system (GRASSBERGER and PROCACCIA, 1983). The average complexity index $\bar{\delta}$ well approximates the correlation dimension. Evaluating the correlation dimension involves slope computation by linear regression. The result highly depends on the scaling range selected for slope computation. This fact evidently shows the advantage of the proposed algorithm over the correlation dimension method.

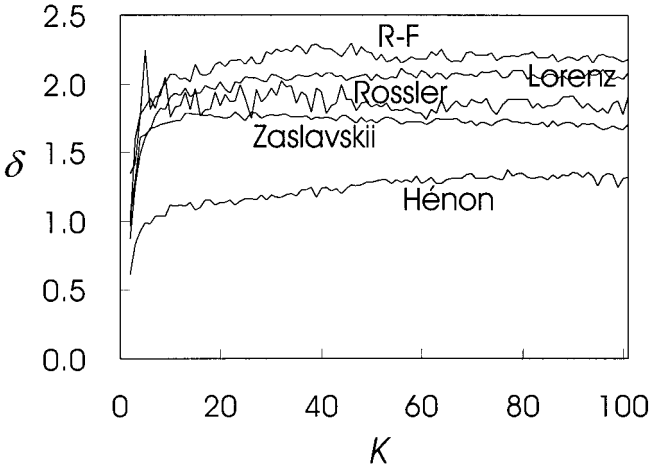


Fig. 1. The computed complexity index (δ) for the five model systems: R-F (Rabinovich-Fabrikant), Lorenz, Rossler, Zaslavskii, and Hénon models, given $1 \leq K \leq 100$

Since the computational time required for δ evaluation highly depends on the evolving length $N$ (number of $n$-dimensional data points), it is a practical consideration to choose the minimum value of $N$ that ensures an adequate coverage of the attractor dynamics. To examine the effect of $N$, complexity index of the Lorenz model is computed for different evolving lengths. Figure 2 displays the $\bar{\delta}$ versus $N$ curves for different $K$ ranges applied to the $\bar{\delta}$ computation. Apparently, pronounced saturation of the curves is observed for $N \geq 2500$. Using an $N$ smaller than 1000 results in a severe underestimation of the complexity index. This may be explained as follows. The Lorenz trajectory is formed by the repetitive process of expansion and contraction. If the analyzed length is not long enough, the evolving orbits may not correctly characterize the global system complexity. Note that the range of values of $K$ shows little effect on $\bar{\delta}$ when $N$ is properly selected ($N \geq 2500$). Deviation is within 3% ($\bar{\delta} = 2.01-2.06$, compared with 2.06 listed in Table 1). This fact demonstrates that $\bar{\delta}$ computation is rather insensitive to a wide range of $K$. It then allows us to confidently select the range of values of $K$ when evaluating the $E\{d_{KNN}\}$ in eq. (12).

Table 1
Average complexity index estimated for five model systems

| | Complexity Index ($\bar{\delta}$) | $N/\Delta t$ | range of $K$ | Correlation Dimension | $N/\Delta t$ |
|---|---|---|---|---|---|
| Rabinovich-Fabrikant model[a] | 2.22 | 8000/0.05 | 30–60 | 2.19 | 15000/0.25 |
| Lorenz model | 2.06 | 8000/0.05 | 30–60 | 2.05 | 15000/0.25 |
| Rossler model | 1.86 | 8000/0.05 | 30–60 | *** | |
| Zaslavskii map | 1.74 | 15000 | 30–60 | ~1.50 | 25000 |
| Hénon map | 1.25 | 15000 | 30–60 | 1.25 | 15000 |

a: The Rabinovich-Fabrikant model is abbreviated to R-F model in Figure 1.

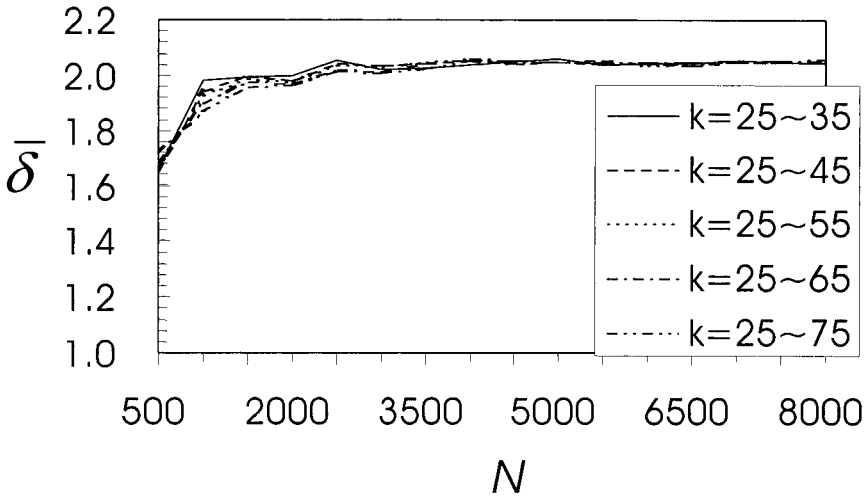


Fig. 2. The $\bar{\delta}$ versus $N$ curves for different $K$ ranges (Lorenz model, $\Delta t = 0.05$)

## 4. Global Complexity Index of Multi-Channel EEG

In this section, we shall first establish a guideline of selecting implementing parameters and then present the numerical results for multi-channel EEG analysis. The EEG data analyzed in this study were recorded from a patient who had an EEG finding of an epilepsy syndrome called "Benign Partial Epilepsy of Childhood", yet had never had obvious epileptic seizures (provided by Dr. Fred Matsuo). The signals exhibit prominent focal-sharp-wave transients characterizing the EEG activities which were generated and spread from the focalized epileptic discharges. A 25-channel electrode array (Figure 3) with a common linked-ear reference was applied in the recording. The signals were digitized by a rate of 200 Hz. Apparently, evaluating the complexity index of multi-channel EEG involves some other factors. They are the number of channels and channel combination. DESTEXHE, SEPULCHRE, and BABLOYANTZ (1988) and DVORAK (1990) proposed to estimate the correlation dimension of multi-channel EEG by using the number of recording sites as embedding dimension of the state space. Following their work, we define the state space dimension $n$ as the number of channels. The channel combination indicates the composition of recording sites used in the analysis. It is associated with the set of state variables describing the brain dynamics. DVORAK (WACKERMANN et al., 1993) showed that the estimated correlation dimension was not significantly affected by array change. We shall present our results of the $\delta$ evaluation in this aspect.

The determination of value of $K$ and length $N$ depends on each other. A 5-channel protocol, involving electrode sites Cz, F3, F4, P3, and P4, is used to study the effect of $K$ and $N$ on $\delta$ computation for EEG. Figure 4 plots the $\delta$ versus $K$ curves for three 20-second EEG segments which only consist of back-

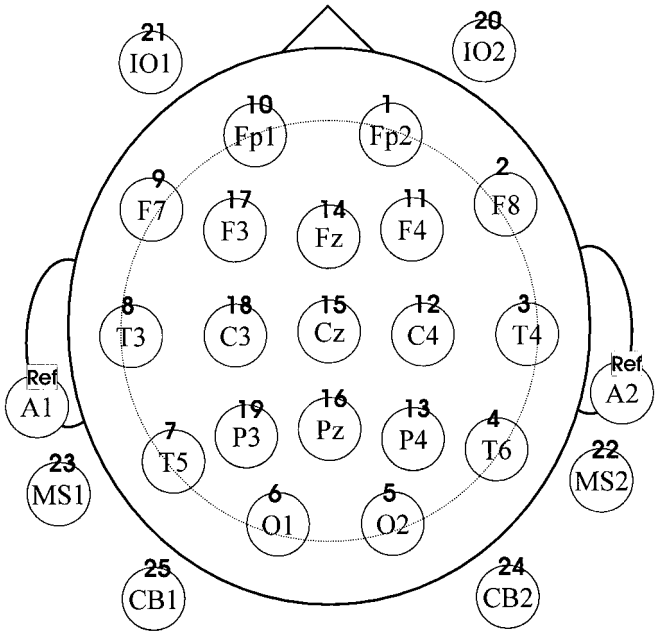


Fig. 3. The 25-channel electrode array applied to the focal-sharp-wave EEG recording

ground activities (no focal-sharp-wave transients). The curves start flattening out at about $K = 20$. The estimated $\delta$ (EEG1: $4.64 \pm 0.09$, EEG2: $4.57 \pm 0.08$, EEG3: $4.73 \pm 0.09$) is fairly consistent in the range of $K \geq 25$. For a small $K$, poor statistics (due to the small number of $n$-dimensional points involved) lead to an unreliable estimate. Yet, in consideration of computational efficiency, a small $K$ is preferred. To study the effect of $N$, the average $\delta$'s ($\bar{\delta}$'s) over several $K$ ranges are computed for values of $N$ ranging from 500 to 4000 stepped by 500 sample points

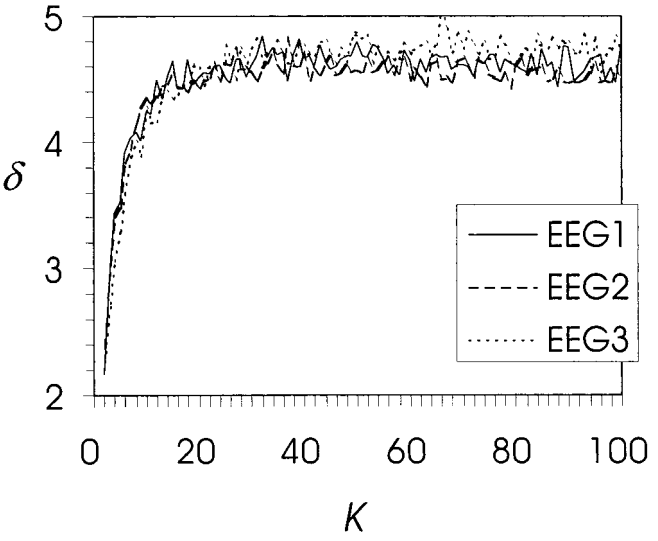


Fig. 4. The $\delta$ versus $K$ curves for three 20-second background EEG sequences

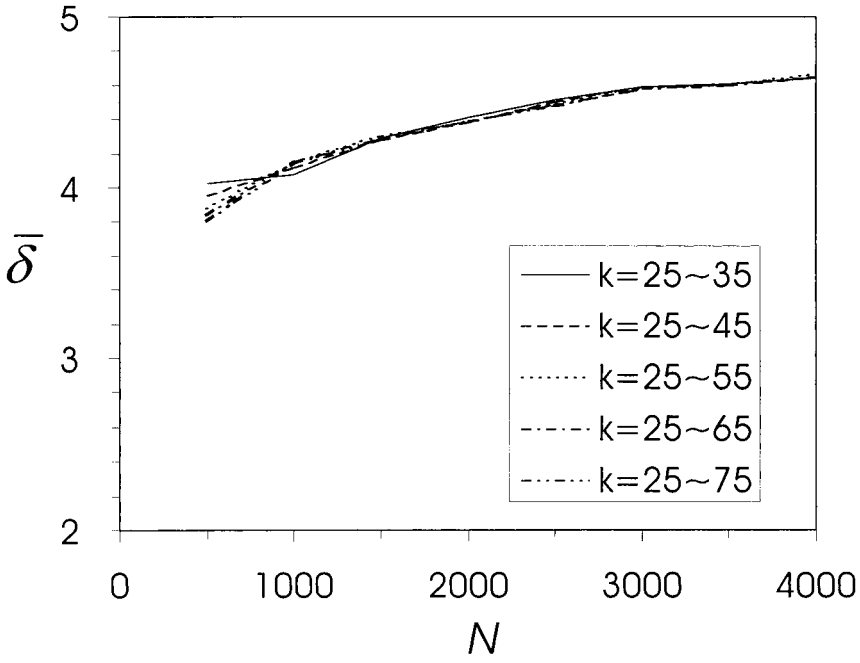


Fig. 5. The $\bar{\delta}$ versus $N$ curves for different $K$ ranges. The values of $N$ range from 500 to 4000 stepped by 500

(Figure 5). Five curves associated with different $K$ ranges well coincide when $N \geq 1000$. Nonetheless, the $\bar{\delta}$ increases with $N$. It cannot be simply imputed to a deficiency of data points. The time-varying characteristics of brain dynamics may cause an increase of complexity index. Unlike the model system (for example, the Lorenz model) governed by a set of fixed parameters, extending the EEG duration often involves changes in brain dynamics. In addition, signal duration required for a reliable and convergent estimate may vary according to different brain states. As a consequence, determining an appropriate length is an intricate task.

When viewing the $\delta$ measure as a relative indicator of the global complexity of EEG waveform patterns, development of the implementing algorithm need not aim at derivation of absolute values. Thus the evolving length $N$ can be much smaller than that required to obtain a convergent estimate, only that it provides an invariant feature descriptor when applied to the long-term EEG monitoring. Figure 6 illustrates the situation. The three curves represent the running measures of $\bar{\delta}$, over a 150-second EEG record, using $N = 1000$ (solid), 1500 (dashed), and 2000 (dotted). In all three cases the moving size is 100 points (0.5 seconds) and the $K$ ranges from 25 to 35. The horizontal axis indicates the beginning time of each running window. The diamonds symbolize the occurrence of focal-sharp-wave events. The three curves basically follow the same up-and-down course. However, we may clearly recognize that increasing the signal duration $N$ results in (time)

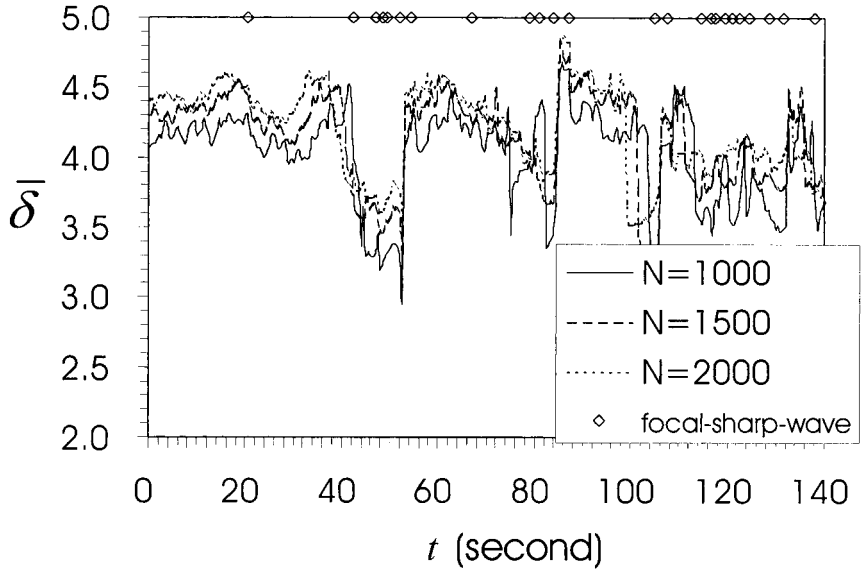


Fig. 6. The running $\bar{\delta}$ computed for a 150-second EEG record. Three different window lengths are used. The moving size is 100 points (0.5 seconds) and the $K$ ranges from 25 to 35

advance and (magnitude) ascent of the running $\bar{\delta}$ curve. The phenomena can be explained as follows. The background EEG has a complexity index between 4.0 and 4.5, which is reduced to $3.0 \sim 3.5$ when focal-sharp-wave transient occurs. Employing a larger window length in the running $\bar{\delta}$ analysis makes the running window earlier encompass the pattern transition in EEG. The ascent of the running $\bar{\delta}$ curve simply reflects the aspect illustrated in Figure 5, in which the computed $\bar{\delta}$ increases with $N$. This analysis demonstrates one of the applications of $\bar{\delta}$ computation to EEG signal. That is, the running $\bar{\delta}$ curve may be used to detect the occurrence of particular events in the EEG monitoring.

As addressed in Section 2, the range of values of $K$ determines the computational efficiency. Large values of $K$ causes heavy computer burden in the competition process. To understand the effect of $K$ range on the running $\bar{\delta}$ analysis, Figure 7 plots the running $\bar{\delta}$ curves for three $K$ ranges, including 25–35 (solid), 25–40 (dashed), and 25–45 (dotted). The running measurement uses a window length of $N = 1000$ (5 seconds) and a moving size of 100 points (0.5 second). All the three curves mostly overlap one another; yet we observe that using the range $25 \leq K \leq 45$ tends to emphasize the transition in EEG activities for this particular EEG record. Extensive study is needed to validate its statistical meaning.

Investigation of the effect of state-space dimension ($n$) is a complicated task since it involves not only the values of $n$ but the composition of electrodes. It is known that, for a deterministic signal, the estimated fractional dimension does not increase with the space dimension (Lo and Principe, 1989). When applying the running $\bar{\delta}$ measurement to the EEG event tracking, computational efficiency be-

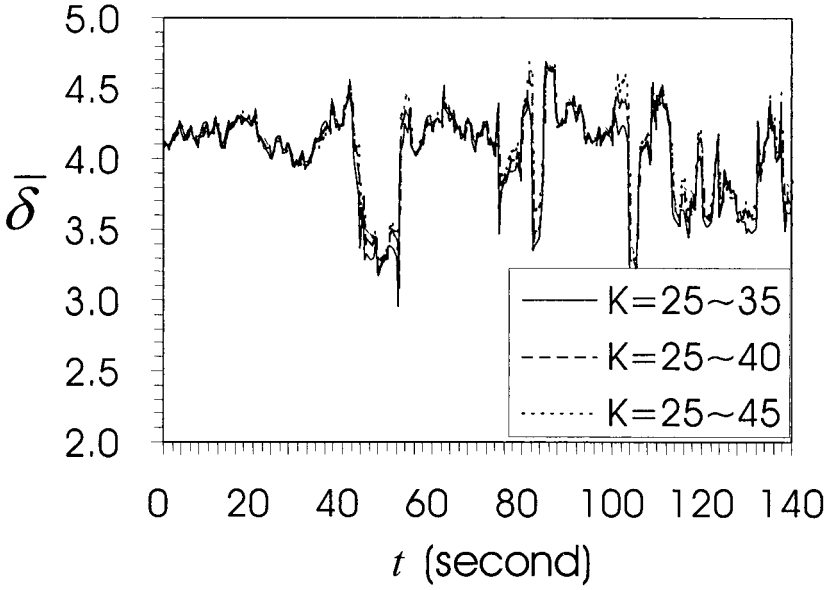


Fig. 7. The running $\bar{\delta}$ curves for three $K$ ranges (window length: 1000, moving size: 100)

comes the major consideration. It is apparent that more computational time is required to analyze the higher-dimensional trajectory. Since nearby EEG channels often record closely correlated brain electric activities (that is, information redundancy exists among multi-channel EEG), a low-dimensional state space is feasible for characterizing the EEG spatial-temporal feature. To illustrate the situation, Figure 8 plots the running $\bar{\delta}$ curves for space dimension $n = 3$, 5, 9, 13, 17, 19, 23, and 25. The

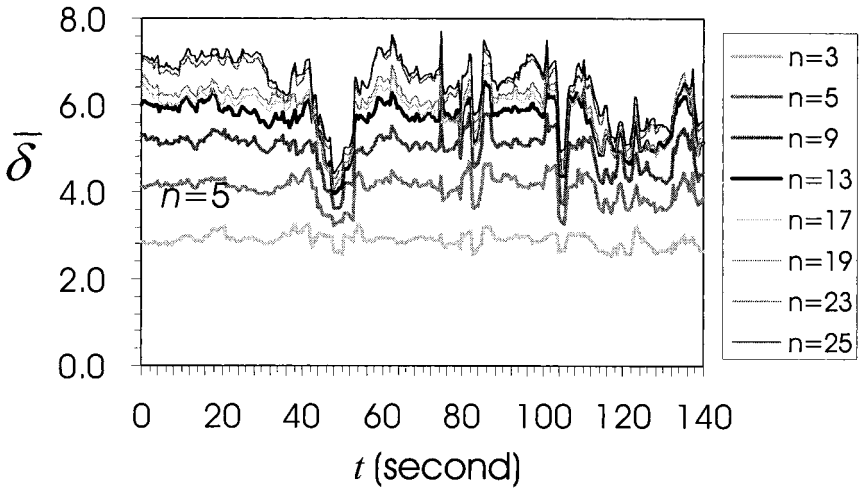


Fig. 8. The running $\bar{\delta}$ curves for different numbers of electrodes (dimensions, $n$) (window length: 1000, moving size: 100, $25 \leq K \leq 35$).

$n$-dimensional electrode array is formed by the first $n$ channels of the totally 25 channels in the order: F3, Cz, F4, P3, P4, F7, F8, T5, T6, Fp1, Fp2, O1, O2, Fz, Pz, C3, C4, T3, T4, IO1, IO2, CB1, CB2, MS1, and MS2. For example, the 9-dimensional trajectory is constructed from the EEG channels F3, Cz, F4, P3, P4, F7, F8, T5, and T6. The group of thicker curves is used to plot the results for $n =$ 3, 5, 9, and 13. As $n$ increases, the running $\bar{\delta}$ curve moves upwards. Nonetheless, it appears to be bounded. The running $\bar{\delta}$ curve exhibits significant change when the value of $n$ increases from 3 to 13 and slightly settles down for values of $n$ between 13 and 19. We may deduce from this phenomenon that the first 13 electrode sites involve sufficient information for quantifying the EEG spatial complexity at this physiological state. In fact, the first 13 electrodes are sparsely distributed over the north-hemispherical (scalp) region (Matsuo, 1991). The additional 6 electrodes (Fz, Pz, C3, C4, T3, and T4) simply fill in between the 13-dimensional electrode array (Figure 3), therefore, result in high information redundancy in the 19-dimensional electrode array. The running $\bar{\delta}$ curve raises again when $n = 23$ because the south-hemispherical electrodes are involved. In consideration of the EEG (focal-sharp-wave) event tracking, the running $\bar{\delta}$ curve for the $n \geq 5$ proves effective, whereas the curve for $n = 3$ fails to identify the events from background EEG. The composition of electrodes is assumed to be the major factor.

Finally, we shall study the effect of electrode array on running $\bar{\delta}$ analysis for a given array size ($n = 5$). Four electrode arrays are used in this study. They include:

array1: Cz F3 F4 P3 P4
array2: Cz Fz Pz C3 C4
array3: Cz F7 F8 T5 T6
array4: Cz Fp1 Fp2 O1 O2

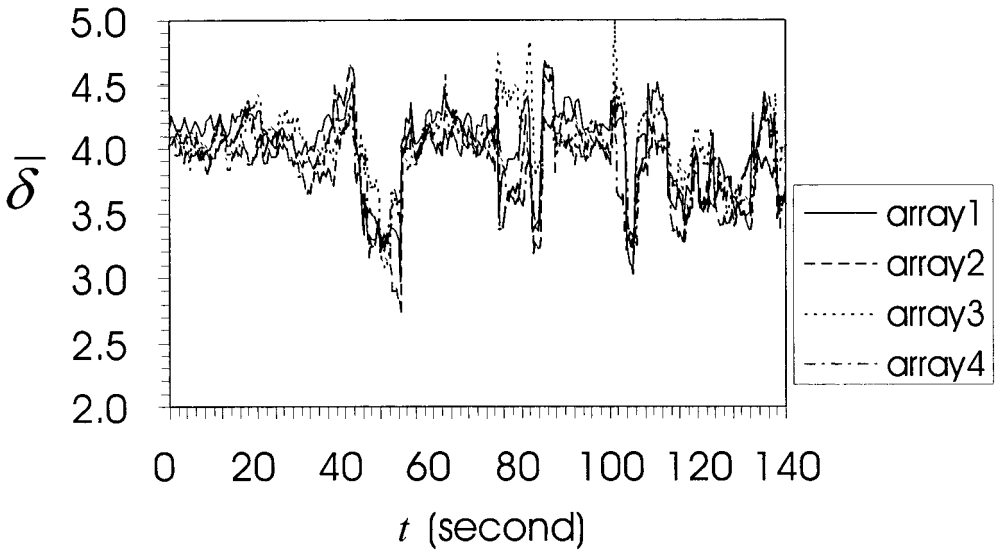


Fig. 9. The running $\bar{\delta}$ curves for four 5-dimension electrode arrays (window length: 1000, moving size: 100, $25 \leq K \leq 35$)

which are all centered on the Cz electrode. Array1 and array2 are composed of nearby electrode sites, while array3 and array4 involve the outer-orbital electrodes. The window length is 1000 and the moving size is 100 sample points. The results plotted in Figure 9 do not exhibit significant statistics associated with the electrode array combination. Note that, during the time interval between the 75th and the 80th second, the running $\bar{\delta}$ curve of array3 rises to the values of $4.1 \sim 4.7$ while the other curves drop to the range of $3.4 \sim 4.0$. In fact, the running $\bar{\delta}$ curve of array3 departs from the others occasionally. The original EEG tracings show that channels F7 and F8 have quite different waveform patterns compared to the other channels used in this analysis. Thus the $\bar{\delta}$ analysis may be a tool to study the spatial correlation in the multi-channel EEG signals.

## 5. Discussion

In this preliminary study, we have introduced the method of estimating intrinsic dimensionality into multi-channel EEG analysis. The work is not aimed at obtaining the absolute value of intrinsic dimensionality, considering the practical use in EEG analysis. Since dimensionality in a sense characterizes the global waveform complexity, we name it the "complexity index ($\delta$)". Evaluation of complexity index is conceptually comprehensible and easily implemented. We have demonstrated the effect of implementing parameters on $\delta$ computation for both model systems and multi-channel EEG. Though selection of implementing parameters affects the computed value of average $\delta$ ($\bar{\delta}$), the running feature of $\bar{\delta}$ appears to be fairly insensitive to a wide range of values of $K$ and $N$. Considering the effect of space dimensions $n$ (number of electrodes), the running $\bar{\delta}$ curve fluctuates in a coherent manner for $n \geq 5$. Analyzing the 5-dimensional (5-channel) EEG trajectory simply requires as few as 1000 data points (5 seconds) for obtaining invariant running $\bar{\delta}$ characteristic. It then resolves the problem of poor temporal resolution and computational inefficiency often encountered in dimensional analysis. According to the analysis of four different electrode arrays, the background EEG has an estimated $\bar{\delta}$ in the range of $4.0 \leq \bar{\delta} \leq 4.5$, which drops to $3.0 \leq \bar{\delta} \leq 3.5$ at the occurrence of the events (focal-sharp-wave activities). The preliminary results presented in this paper demonstrate that this method has the potential value to quantification of EEG spatial correlation and identification of EEG pattern transition.

## Acknowledgements

The authors would like to thank Dr. F. Matsuo of the Department of Neurology, University of Utah Medical School for providing the focal-sharp-wave EEG data for this research work.

*References*

BABLOYANTZ, A. and DESTEXHE, A., 1986: Low-dimensional chaos in an instance of epilepsy. *Proc. Nat. Acad. Sci. USA* **83**, 3513–3517.

BRUSKE, J. and SOMMER G., 1998: Intrinsic dimensionality estimation with optimally topology preserving maps. *IEEE Trans. Patt. Anal. Machine Intell.* **20** (5), 572–575.

DESTEXHE, A., SEPULCHRE, J. A., and BABLOYANTZ, A., 1988: A comparative study of the experimental quantification of deterministic chaos. *Phys. Lett.* **A132**, 101–106.

DVORAK, I., 1990: Takens versus multichannel reconstruction in EEG correlation exponent estimations. *Phys. Lett.* **A151**, 225–233.

FRASER, D. A. S., 1957: *Nonparametric Methods in Statistics*. New York, Wiley, ch. 4.

FUKUNAGA, K. and FLICK, T. E., 1984: Classification error for a very large number of classes. *IEEE Trans. Patt. Anal. Machine Intell.* PAMI-6 (6), 779–788.

FUKUNAGA, K. and OLSEN, D. R., 1971: An algorithm for finding intrinsic dimensionality of data. *IEEE Trans. Comput.* C-20, 176–183.

GRASSBERGER, P. and PROCACCIA, I., 1983: Characterization of strange attractors. *Phys. Rev. Lett.* **50** (5), 346–349.

HENTSCHEL, H. G. E. and PROCACCIA, I., 1983: The infinite number of generalized dimensions of fractals and strange attractors. *Physica* **8**D, 435–444.

LO, P.-C. and PRINCIPE, J. C., 1989: Dimensionality analysis of EEG segments: Experimental considerations. *Proc. Int. Joint Conf. Of the Neural Network Soc.,* 693–698.

MATSUO, F., 1991: Expanded head surface EEG electrode array: An application to display the voltage topography of focal epileptiform discharges of mesiotemporal origin. *J. Clin. Neurophysiol.* **8** (4), 442–451.

MICHEL, O. and FLANDRIN, P., 1993: Local minimum redundancy representation of a system for estimating the number of its degrees of freedom. *IEEE Signal Proc. Workshop on Higher-order Statistics*, 341–345.

PASSAMANTE, A. and FARRELL, M. E., 1991: Characterizing attractors using local intrinsic dimension via higher-order statistics. *Phys. Rev.* **A43** (10), 5268–5274.

PETTIS, K. W., BAILEY, T. A., JAIN, A. K., and DUBES, R. C., 1979: An intrinsic dimensionality estimator from near-neighbor information. *IEEE Trans. Patt. Anal. Machine Intell.* PAMI-1, 25–37.

PIJN, J. P. M., NEERVEN, J. V., NOEST, A., and LOPES DA SILVA, F. H., 1991: Chaos or noise in EEG signals: Dependence on state and brain site. *Electroenceph. Clin. Neurophysiol.* **79**, 371–381.

RAPP, P. E., BASHORE, T. R., MARTINERIE, J. M., ALBANO, A. M., and MEES, A. I., 1989: Dynamics of brain electrical activity. *Brain Topography* **2**, 99–118.

VAN GILS, M., ROSENFALCK, A., WHITE, S., PRIOR, P., GADE, J., SENHADJI, L., THOMSEN, C., GHOSH, I. R., LANGFORD, R. M., and JENSEN, K., 1997: Signal processing in prolonged EEG recordings during intensive care. *IEEE Eng. in Medicine & Biology* **16** (6), 56–63.

VERVEER, P. J. and DUIN, P. W., 1995: An evaluation of intrinsic dimensionality estimators. *IEEE Trans. Patt. Anal. Machine Intell.* **17** (1), 81–86.

WACKERMANN J., LEHMANN, D., DVORAK, I., and MICHEL, C. M., 1993: Global dimensional complexity of multi-channel EEG indicates change of human brain functional state after a single dose of a nootropic drug. *Electroenceph. Clin. Neurophysiol.* **86**, 193–198.

YAYLALI, I., KOÇAK, H., and JAYAKAR, P., 1996: Detection of seizures from small samples using nonlinear dynamic system theory. *IEEE Trans. Biomed. Eng.* **43** (7), 743–751.

Dr. PEI-CHEN LO
Department of Electrical and Control Engineering
National Chiao Tung University
1001 Ta-Hsueh Road
Hsinchu 30010, Taiwan
Republic of China
Email: pclo@cc.nctu.edu.tw

Received, August 1999
Revised, June 2000
Accepted, July 2000